

# Measurement of the Inclusive Electron Neutrino Charged Current Cross Section on Carbon with the T2K Near Detector

K. Abe,<sup>46</sup> J. Adam,<sup>32</sup> H. Aihara,<sup>45,23</sup> T. Akiri,<sup>9</sup> C. Andreopoulos,<sup>44</sup> S. Aoki,<sup>24</sup> A. Ariga,<sup>2</sup> S. Assylbekov,<sup>8</sup> D. Autiero,<sup>29</sup> M. Barbi,<sup>39</sup> G.J. Barker,<sup>54</sup> G. Barr,<sup>35</sup> M. Bass,<sup>8</sup> M. Batkiewicz,<sup>13</sup> F. Bay,<sup>11</sup> V. Berardi,<sup>18</sup> B.E. Berger,<sup>8,23</sup> S. Berkman,<sup>4</sup> S. Bhadra,<sup>58</sup> F.d.M. Blaszczyk,<sup>28</sup> A. Blondel,<sup>12</sup> C. Bojecho,<sup>51</sup> S. Bordoni,<sup>15</sup> S.B. Boyd,<sup>54</sup> D. Brailsford,<sup>17</sup> A. Bravar,<sup>12</sup> C. Bronner,<sup>23</sup> N. Buchanan,<sup>8</sup> R.G. Calland,<sup>27</sup> J. Caravaca Rodríguez,<sup>15</sup> S.L. Cartwright,<sup>42</sup> R. Castillo,<sup>15</sup> M.G. Catanesi,<sup>18</sup> A. Cervera,<sup>16</sup> D. Cherdack,<sup>8</sup> G. Christodoulou,<sup>27</sup> A. Clifton,<sup>8</sup> J. Coleman,<sup>27</sup> S.J. Coleman,<sup>7</sup> G. Collazuol,<sup>20</sup> K. Connolly,<sup>55</sup> L. Cremonesi,<sup>38</sup> A. Dabrowska,<sup>13</sup> I. Danko,<sup>37</sup> R. Das,<sup>8</sup> S. Davis,<sup>55</sup> P. de Perio,<sup>49</sup> G. De Rosa,<sup>19</sup> T. Dealtry,<sup>44,35</sup> S.R. Dennis,<sup>54,44</sup> C. Densham,<sup>44</sup> D. Dewhurst,<sup>35</sup> F. Di Lodovico,<sup>38</sup> S. Di Luise,<sup>11</sup> O. Drapier,<sup>10</sup> T. Duboyski,<sup>38</sup> K. Duffy,<sup>35</sup> J. Dumarchez,<sup>36</sup> S. Dytman,<sup>37</sup> M. Dziewiecki,<sup>53</sup> S. Emery-Schrenk,<sup>6</sup> A. Ereditato,<sup>2</sup> L. Escudero,<sup>16</sup> A.J. Finch,<sup>26</sup> M. Friend,<sup>14,\*</sup> Y. Fujii,<sup>14,\*</sup> Y. Fukuda,<sup>30</sup> A.P. Furmanski,<sup>54</sup> V. Galymov,<sup>29</sup> S. Giffin,<sup>39</sup> C. Giganti,<sup>36</sup> K. Gilje,<sup>32</sup> D. Goeldi,<sup>2</sup> T. Golan,<sup>57</sup> M. Gonin,<sup>10</sup> N. Grant,<sup>26</sup> D. Gudin,<sup>22</sup> D.R. Hadley,<sup>54</sup> A. Haesler,<sup>12</sup> M.D. Haigh,<sup>54</sup> P. Hamilton,<sup>17</sup> D. Hansen,<sup>37</sup> T. Hara,<sup>24</sup> M. Hartz,<sup>23,50</sup> T. Hasegawa,<sup>14,\*</sup> N.C. Hastings,<sup>39</sup> Y. Hayato,<sup>46,23</sup> C. Hearty,<sup>4,†</sup> R.L. Helmer,<sup>50</sup> M. Hierholzer,<sup>2</sup> J. Hignight,<sup>32</sup> A. Hillairet,<sup>51</sup> A. Himmel,<sup>9</sup> T. Hiraki,<sup>25</sup> S. Hirota,<sup>25</sup> J. Holeczek,<sup>43</sup> S. Horikawa,<sup>11</sup> K. Huang,<sup>25</sup> A.K. Ichikawa,<sup>25</sup> K. Ieki,<sup>25</sup> M. Ieva,<sup>15</sup> M. Ikeda,<sup>46</sup> J. Imber,<sup>32</sup> J. Insler,<sup>28</sup> T.J. Irvine,<sup>47</sup> T. Ishida,<sup>14,\*</sup> T. Ishii,<sup>14,\*</sup> E. Iwai,<sup>14</sup> K. Iwamoto,<sup>40</sup> K. Iyogi,<sup>46</sup> A. Izmaylov,<sup>16,22</sup> A. Jacob,<sup>35</sup> B. Jamieson,<sup>56</sup> R.A. Johnson,<sup>7</sup> J.H. Jo,<sup>32</sup> P. Jonsson,<sup>17</sup> C.K. Jung,<sup>32,‡</sup> M. Kabirnezhad,<sup>31</sup> A.C. Kaboth,<sup>17</sup> T. Kajita,<sup>47,‡</sup> H. Kakuno,<sup>48</sup> J. Kameda,<sup>46</sup> Y. Kanazawa,<sup>45</sup> D. Karlen,<sup>51,50</sup> I. Karpikov,<sup>22</sup> T. Katori,<sup>38</sup> E. Kearns,<sup>3,23,‡</sup> M. Khabibullin,<sup>22</sup> A. Khotjantsev,<sup>22</sup> D. Kielczewska,<sup>52</sup> T. Kikawa,<sup>25</sup> A. Kilinski,<sup>31</sup> J. Kim,<sup>4</sup> J. Kisiel,<sup>43</sup> P. Kitching,<sup>1</sup> T. Kobayashi,<sup>14,\*</sup> L. Koch,<sup>41</sup> A. Kolaceke,<sup>39</sup> A. Konaka,<sup>50</sup> L.L. Kormos,<sup>26</sup> A. Korzenev,<sup>12</sup> Y. Koshio,<sup>33,‡</sup> W. Kropp,<sup>5</sup> H. Kubo,<sup>25</sup> Y. Kudenko,<sup>22,§</sup> R. Kurjata,<sup>53</sup> T. Kutter,<sup>28</sup> J. Lagoda,<sup>31</sup> I. Lamont,<sup>26</sup> E. Larkin,<sup>54</sup> M. Laveder,<sup>20</sup> M. Lawe,<sup>42</sup> M. Lazos,<sup>27</sup> T. Lindner,<sup>50</sup> C. Lister,<sup>54</sup> R.P. Litchfield,<sup>54</sup> A. Longhin,<sup>20</sup> L. Ludovici,<sup>21</sup> L. Magaletti,<sup>18</sup> K. Mahn,<sup>50</sup> M. Malek,<sup>17</sup> S. Manly,<sup>40</sup> A.D. Marino,<sup>7</sup> J. Marteau,<sup>29</sup> J.F. Martin,<sup>49</sup> S. Martynenko,<sup>22</sup> T. Maruyama,<sup>14,\*</sup> V. Matveev,<sup>22</sup> K. Mavrokoridis,<sup>27</sup> E. Mazzucato,<sup>6</sup> M. McCarthy,<sup>4</sup> N. McCauley,<sup>27</sup> K.S. McFarland,<sup>40</sup> C. McGrew,<sup>32</sup> C. Metelko,<sup>27</sup> P. Mijakowski,<sup>31</sup> C.A. Miller,<sup>50</sup> A. Minamino,<sup>25</sup> O. Mineev,<sup>22</sup> A. Missert,<sup>7</sup> M. Miura,<sup>46,‡</sup> S. Moriyama,<sup>46,‡</sup> Th.A. Mueller,<sup>10</sup> A. Murakami,<sup>25</sup> M. Murdoch,<sup>27</sup> S. Murphy,<sup>11</sup> J. Myslik,<sup>51</sup> T. Nakadaira,<sup>14,\*</sup> M. Nakahata,<sup>46,23</sup> K. Nakamura,<sup>23,14,\*</sup> S. Nakayama,<sup>46,‡</sup> T. Nakaya,<sup>25,23</sup> K. Nakayoshi,<sup>14,\*</sup> C. Nielsen,<sup>4</sup> M. Nirkko,<sup>2</sup> K. Nishikawa,<sup>14,\*</sup> Y. Nishimura,<sup>47</sup> H.M. O'Keefe,<sup>26</sup> R. Ohta,<sup>14,\*</sup> K. Okumura,<sup>47,23</sup> T. Okusawa,<sup>34</sup> W. Oryszczak,<sup>52</sup> S.M. Oser,<sup>4</sup> R.A. Owen,<sup>38</sup> Y. Oyama,<sup>14,\*</sup> V. Palladino,<sup>19</sup> J.L. Palomino,<sup>32</sup> V. Paolone,<sup>37</sup> D. Payne,<sup>27</sup> O. Perevozchikov,<sup>28</sup> J.D. Perkin,<sup>42</sup> Y. Petrov,<sup>4</sup> L. Pickard,<sup>42</sup> E.S. Pinzon Guerra,<sup>58</sup> C. Pistillo,<sup>2</sup> P. Plonski,<sup>53</sup> E. Poplawska,<sup>38</sup> B. Popov,<sup>36,¶</sup> M. Posiadala,<sup>52</sup> J.-M. Poutissou,<sup>50</sup> R. Poutissou,<sup>50</sup> P. Przewlocki,<sup>31</sup> B. Quilain,<sup>10</sup> E. Radicioni,<sup>18</sup> P.N. Ratoff,<sup>26</sup> M. Ravonel,<sup>12</sup> M.A.M. Rayner,<sup>12</sup> A. Redij,<sup>2</sup> M. Reeves,<sup>26</sup> E. Reinherz-Aronis,<sup>8</sup> P.A. Rodrigues,<sup>40</sup> P. Rojas,<sup>8</sup> E. Rondio,<sup>31</sup> S. Roth,<sup>41</sup> A. Rubbia,<sup>11</sup> D. Ruterbories,<sup>40</sup> R. Sacco,<sup>38</sup> K. Sakashita,<sup>14,\*</sup> F. Sánchez,<sup>15</sup> F. Sato,<sup>14</sup> E. Scantamburlo,<sup>12</sup> K. Scholberg,<sup>9,‡</sup> S. Schoppmann,<sup>41</sup> J. Schwehr,<sup>8</sup> M. Scott,<sup>50</sup> Y. Seiya,<sup>34</sup> T. Sekiguchi,<sup>14,\*</sup> H. Sekiya,<sup>46,‡</sup> D. Sgalaberna,<sup>11</sup> M. Shiozawa,<sup>46,23</sup> S. Short,<sup>38</sup> Y. Shustrov,<sup>22</sup> P. Sinclair,<sup>17</sup> B. Smith,<sup>17</sup> M. Smy,<sup>5</sup> J.T. Sobczyk,<sup>57</sup> H. Sobel,<sup>5,23</sup> M. Sorel,<sup>16</sup> L. Southwell,<sup>26</sup> P. Stamoulis,<sup>16</sup> J. Steinmann,<sup>41</sup> B. Still,<sup>38</sup> Y. Suda,<sup>45</sup> A. Suzuki,<sup>24</sup> K. Suzuki,<sup>25</sup> S.Y. Suzuki,<sup>14,\*</sup> Y. Suzuki,<sup>23,23</sup> R. Tacik,<sup>39,50</sup> M. Tada,<sup>14,\*</sup> S. Takahashi,<sup>25</sup> A. Takeda,<sup>46</sup> Y. Takeuchi,<sup>24,23</sup> H.K. Tanaka,<sup>46,‡</sup> H.A. Tanaka,<sup>4,†</sup> M.M. Tanaka,<sup>14,\*</sup> D. Terhorst,<sup>41</sup> R. Terri,<sup>38</sup> L.F. Thompson,<sup>42</sup> A. Thorley,<sup>27</sup> S. Tobayama,<sup>4</sup> W. Toki,<sup>8</sup> T. Tomura,<sup>46</sup> Y. Totsuka,<sup>\*\*</sup> C. Touramanis,<sup>27</sup> T. Tsukamoto,<sup>14,\*</sup> M. Tzanov,<sup>28</sup> Y. Uchida,<sup>17</sup> A. Vacheret,<sup>35</sup> M. Vagins,<sup>23,5</sup> G. Vasseur,<sup>6</sup> T. Wachala,<sup>13</sup> A.V. Waldron,<sup>35</sup> C.W. Walter,<sup>9,‡</sup> D. Wark,<sup>44,17</sup> M.O. Wascko,<sup>17</sup> A. Weber,<sup>44,35</sup> R. Wendell,<sup>46,‡</sup> R.J. Wilkes,<sup>55</sup> M.J. Wilking,<sup>50</sup> C. Wilkinson,<sup>42</sup> Z. Williamson,<sup>35</sup> J.R. Wilson,<sup>38</sup> R.J. Wilson,<sup>8</sup> T. Wongjirad,<sup>9</sup> Y. Yamada,<sup>14,\*</sup> K. Yamamoto,<sup>34</sup> C. Yanagisawa,<sup>32,††</sup> T. Yano,<sup>24</sup> S. Yen,<sup>50</sup> N. Yershov,<sup>22</sup> M. Yokoyama,<sup>45,‡</sup> T. Yuan,<sup>7</sup> M. Yu,<sup>58</sup> A. Zalewska,<sup>13</sup> J. Zalipska,<sup>31</sup> L. Zambelli,<sup>14,\*</sup> K. Zaremba,<sup>53</sup> M. Ziembicki,<sup>53</sup> E.D. Zimmerman,<sup>7</sup> M. Zito,<sup>6</sup> and J. Żmuda<sup>57</sup>

(The T2K Collaboration)

<sup>1</sup> University of Alberta, Centre for Particle Physics, Department of Physics, Edmonton, Alberta, Canada

<sup>2</sup> University of Bern, Albert Einstein Center for Fundamental Physics, Laboratory for High Energy Physics (LHEP), Bern, Switzerland

<sup>3</sup> Boston University, Department of Physics, Boston, Massachusetts, U.S.A.

<sup>4</sup> University of British Columbia, Department of Physics and Astronomy, Vancouver, British Columbia, Canada

- <sup>5</sup>University of California, Irvine, Department of Physics and Astronomy, Irvine, California, U.S.A.  
<sup>6</sup>IRFU, CEA Saclay, Gif-sur-Yvette, France
- <sup>7</sup>University of Colorado at Boulder, Department of Physics, Boulder, Colorado, U.S.A.  
<sup>8</sup>Colorado State University, Department of Physics, Fort Collins, Colorado, U.S.A.  
<sup>9</sup>Duke University, Department of Physics, Durham, North Carolina, U.S.A.
- <sup>10</sup>Ecole Polytechnique, IN2P3-CNRS, Laboratoire Leprince-Ringuet, Palaiseau, France  
<sup>11</sup>ETH Zurich, Institute for Particle Physics, Zurich, Switzerland  
<sup>12</sup>University of Geneva, Section de Physique, DPNC, Geneva, Switzerland  
<sup>13</sup>H. Niewodniczanski Institute of Nuclear Physics PAN, Cracow, Poland
- <sup>14</sup>High Energy Accelerator Research Organization (KEK), Tsukuba, Ibaraki, Japan  
<sup>15</sup>Institut de Fisica d'Altes Energies (IFAE), Bellaterra (Barcelona), Spain  
<sup>16</sup>IFIC (CSIC & University of Valencia), Valencia, Spain  
<sup>17</sup>Imperial College London, Department of Physics, London, United Kingdom
- <sup>18</sup>INFN Sezione di Bari and Università e Politecnico di Bari, Dipartimento Interuniversitario di Fisica, Bari, Italy  
<sup>19</sup>INFN Sezione di Napoli and Università di Napoli, Dipartimento di Fisica, Napoli, Italy  
<sup>20</sup>INFN Sezione di Padova and Università di Padova, Dipartimento di Fisica, Padova, Italy  
<sup>21</sup>INFN Sezione di Roma and Università di Roma "La Sapienza", Roma, Italy  
<sup>22</sup>Institute for Nuclear Research of the Russian Academy of Sciences, Moscow, Russia  
<sup>23</sup>Kavli Institute for the Physics and Mathematics of the Universe (WPI),  
 Todai Institutes for Advanced Study, University of Tokyo, Kashiwa, Chiba, Japan  
<sup>24</sup>Kobe University, Kobe, Japan  
<sup>25</sup>Kyoto University, Department of Physics, Kyoto, Japan  
<sup>26</sup>Lancaster University, Physics Department, Lancaster, United Kingdom  
<sup>27</sup>University of Liverpool, Department of Physics, Liverpool, United Kingdom
- <sup>28</sup>Louisiana State University, Department of Physics and Astronomy, Baton Rouge, Louisiana, U.S.A.  
<sup>29</sup>Université de Lyon, Université Claude Bernard Lyon 1, IPN Lyon (IN2P3), Villeurbanne, France  
<sup>30</sup>Miyagi University of Education, Department of Physics, Sendai, Japan  
<sup>31</sup>National Centre for Nuclear Research, Warsaw, Poland
- <sup>32</sup>State University of New York at Stony Brook, Department of Physics and Astronomy, Stony Brook, New York, U.S.A.  
<sup>33</sup>Okayama University, Department of Physics, Okayama, Japan  
<sup>34</sup>Osaka City University, Department of Physics, Osaka, Japan  
<sup>35</sup>Oxford University, Department of Physics, Oxford, United Kingdom  
<sup>36</sup>UPMC, Université Paris Diderot, CNRS/IN2P3, Laboratoire de  
 Physique Nucléaire et de Hautes Energies (LPNHE), Paris, France
- <sup>37</sup>University of Pittsburgh, Department of Physics and Astronomy, Pittsburgh, Pennsylvania, U.S.A.  
<sup>38</sup>Queen Mary University of London, School of Physics and Astronomy, London, United Kingdom  
<sup>39</sup>University of Regina, Department of Physics, Regina, Saskatchewan, Canada  
<sup>40</sup>University of Rochester, Department of Physics and Astronomy, Rochester, New York, U.S.A.  
<sup>41</sup>RWTH Aachen University, III. Physikalisches Institut, Aachen, Germany  
<sup>42</sup>University of Sheffield, Department of Physics and Astronomy, Sheffield, United Kingdom  
<sup>43</sup>University of Silesia, Institute of Physics, Katowice, Poland
- <sup>44</sup>STFC, Rutherford Appleton Laboratory, Harwell Oxford, and Daresbury Laboratory, Warrington, United Kingdom  
<sup>45</sup>University of Tokyo, Department of Physics, Tokyo, Japan  
<sup>46</sup>University of Tokyo, Institute for Cosmic Ray Research, Kamioka Observatory, Kamioka, Japan  
<sup>47</sup>University of Tokyo, Institute for Cosmic Ray Research, Research Center for Cosmic Neutrinos, Kashiwa, Japan  
<sup>48</sup>Tokyo Metropolitan University, Department of Physics, Tokyo, Japan  
<sup>49</sup>University of Toronto, Department of Physics, Toronto, Ontario, Canada  
<sup>50</sup>TRIUMF, Vancouver, British Columbia, Canada
- <sup>51</sup>University of Victoria, Department of Physics and Astronomy, Victoria, British Columbia, Canada  
<sup>52</sup>University of Warsaw, Faculty of Physics, Warsaw, Poland  
<sup>53</sup>Warsaw University of Technology, Institute of Radioelectronics, Warsaw, Poland  
<sup>54</sup>University of Warwick, Department of Physics, Coventry, United Kingdom  
<sup>55</sup>University of Washington, Department of Physics, Seattle, Washington, U.S.A.  
<sup>56</sup>University of Winnipeg, Department of Physics, Winnipeg, Manitoba, Canada  
<sup>57</sup>Wroclaw University, Faculty of Physics and Astronomy, Wroclaw, Poland  
<sup>58</sup>York University, Department of Physics and Astronomy, Toronto, Ontario, Canada

(Dated: August 1, 2014)

The T2K off-axis near detector, ND280, is used to make the first differential cross-section measurements of electron neutrino charged current interactions at energies  $\sim 1$  GeV as a function of electron momentum, electron scattering angle and four-momentum transfer of the interaction. The total flux-averaged  $\nu_e$  charged current cross-section on carbon is measured to be  $\langle\sigma\rangle_\phi = 1.11 \pm 0.09$  (stat)  $\pm 0.18$  (syst)  $\times 10^{-38}$  cm<sup>2</sup>/nucleon. The differential and total cross-section measurements agree with the predictions of two leading neutrino interaction generators,

NEUT and GENIE. The NEUT prediction is  $1.23 \times 10^{-38}$  cm<sup>2</sup>/nucleon and the GENIE prediction is  $1.08 \times 10^{-38}$  cm<sup>2</sup>/nucleon. The total  $\nu_e$  charged current cross-section result is also in agreement with data from the Gargamelle experiment.

PACS numbers: 14.60.Pq, 14.60.Lm, 25.30.Pt, 29.40.Ka

*Introduction*—T2K is a long baseline neutrino oscillation experiment measuring  $\nu_e$  appearance and  $\nu_\mu$  disappearance from a  $\nu_\mu$  beam. Neutrino oscillations are described by a mixing matrix parametrized by three mixing angles and a CP violating phase,  $\delta_{\text{CP}}$  [1, 2]. The three mixing angles have been measured to better than 10% precision [3], and measuring  $\delta_{\text{CP}}$  is currently a major goal in neutrino physics [4].

Future  $\nu_e$  appearance measurements can be used to search for CP violation in neutrino interactions, and these rely on precise understanding of both  $\nu_\mu$  and  $\nu_e$  charged-current (CC) interaction cross-sections at energies  $\sim 1$  GeV. Many  $\nu_\mu$  cross-section measurements have been made at the GeV scale, both of the total CC inclusive cross-section and of individual interaction modes (see Ref. [5] for a review of cross-section data, and Refs. [6–8] for recent results). Only the Gargamelle experiment has measured the  $\nu_e$  CC inclusive cross-section at the GeV scale [9], and there are currently no  $\nu_e$  differential cross-section results as a function of the electron kinematics. Theoretical differences are expected between  $\nu_e$  and  $\nu_\mu$  cross-sections [10], and measuring these with data is critical to understand the systematic uncertainties related to the search for CP violation in the lepton sector. The uncertainty in  $\nu_e$  cross-sections will become increasingly important in future oscillation experiments as statistical and other systematic uncertainties are reduced.

In this Letter we present the first  $\nu_e$  CC inclusive differential cross-section measurements for neutrinos with energy  $\sim 1$  GeV as a function of the electron momentum ( $p_e$ ), electron scattering angle ( $\cos(\theta_e)$ ) and the four-momentum transfer of the interaction ( $Q^2$ ). The total flux-averaged CC inclusive cross-section is also presented.

*T2K Experiment*—T2K [11] operates from the J-PARC facility in Tokai, Japan. A muon neutrino beam is produced from the decay of charged pions and kaons generated by 30 GeV proton collisions on a graphite target and focused by three magnetic horns. Downstream of the horns is the decay volume, 96 meters in length, followed by the beam dump and muon monitors (MUMON [12]). The neutrino beam illuminates an on-axis near detector (INGRID [13]), an off-axis near detector (ND280) and an off-axis far detector (Super-Kamiokande [14]). The off-axis detectors are positioned at an angle of  $2.5^\circ$  relative to the beam axis direction. The near detectors are located 280 meters from the target and are used to determine the neutrino beam direction, spectrum, and composition before oscillations, and to measure neutrino cross-sections. Super-Kamiokande, a 50 kt water Cherenkov detector sit-

uated 295 km away, is used to detect the neutrinos after oscillation.

ND280 is a magnetized multi-purpose detector designed to measure interactions of both  $\nu_\mu$  and  $\nu_e$  from the T2K beam before oscillations. It is composed of a number of subdetectors installed inside the refurbished UA1/NOMAD magnet, which provides a magnetic field of 0.2 T. The central subdetectors form a tracking detector, composed of two fine-grained scintillator detectors (FGDs [15]) and three time projection chambers (TPCs [16]). The FGDs are used as the target for the neutrino interactions, and while the upstream FGD (FGD1) is composed solely of scintillator bars, the downstream FGD (FGD2) also contains water layers. Upstream of the tracker is a  $\pi^0$  detector (P0D [17]), explicitly built to measure neutrino interactions with a  $\pi^0$  in the final state. The tracker and P0D are surrounded by a set of electromagnetic calorimeters (ECals [18]), and the magnet yokes are instrumented with side muon range detectors (SMRDs [19]) to track high angle muons.

The results presented here are based on data taken from January 2010 to May 2013. During this period the proton beam power has steadily increased and reached 220 kW continuous operation with a world record of  $1.2 \times 10^{14}$  protons per pulse. The physics-quality data for this analysis corresponds to a total of  $5.90 \times 10^{20}$  protons on target (p.o.t.).

*Neutrino Beam Flux*—The neutrino beam flux [20] is predicted by modeling interactions of the primary beam protons with a graphite target using the FLUKA2008 package [21] and external hadron production data from the CERN NA61/SHINE experiment [22, 23]. GEANT3 [24] with GCALOR [25] is used to simulate the propagation of secondary and tertiary pions and kaons, and their decays into neutrinos. Decays of kaons and muons, in the decay volume, create the approximately 1%  $\nu_e$  component of the beam. Muon decays are the dominant source of  $\nu_e$  with energies below 1 GeV, with higher energy neutrinos produced by kaon decays.

The neutrino flux uncertainties are dominated by hadron production uncertainties, with contributions from the neutrino beam direction and the proton beam uncertainties. The neutrino beam direction—monitored indirectly by MUMON on a spill-by-spill basis, and directly by INGRID [26]—has been well within the required  $\pm 1$  mrad during the full run period. The neutrino interaction rate per p.o.t. has also been measured by INGRID, and is stable within 0.7%. The total systematic uncertainty on the  $\nu_e$  flux is 13% at the mean  $\nu_e$  energy (1.3 GeV).

*Selection of Electron Neutrino Interactions in ND280*—Full details of the event selections can be found in Ref. [27], where the only difference is that in this analysis only interactions in FGD1 are selected, rather than FGD1 and FGD2. This is so that interactions on water in FGD2 are not included.

Electron neutrino interactions are selected using the highest momentum negative track starting inside the fiducial volume of FGD1. To reduce the large background from  $\nu_\mu$  charged current interactions, electron particle identification criteria are applied using TPC  $dE/dx$  and ECal shape and energy measurements. These remove 99.9% of  $\mu^-$  tracks, and although a clean sample of  $e^-$  is selected, 62.4% of events are from photons which produce  $e^+e^-$  pairs in FGD1. This  $\gamma$  background is reduced by searching for a positron and applying an invariant mass cut, and vetoing on activity in TPC1, the P0D, and ECals upstream of FGD1. After this procedure, 315  $\nu_e$  CC interaction candidates are selected, with an expected purity of 65%. The reconstructed momentum, scattering angle, and  $Q^2$  distributions are shown in Fig. 1, and compared to the prediction from the NEUT neutrino interaction generator [28].  $Q^2$  is reconstructed assuming CC quasi-elastic (CCQE) kinematics [29], with a stationary target nucleon and 25 MeV binding energy.

The background from  $\gamma \rightarrow e^+e^-$  conversions in the  $\nu_e$  sample is 23%, 70% of which are from neutrinos interactions outside the FGD1 fiducial volume. A control sample, referred to as the  $\gamma$  sample, is used to constrain this, and is selected by finding electron-positron pairs that enter the TPC and that have a low invariant mass. The data shows a deficit at low momentum in both the  $\nu_e$  and  $\gamma$  samples. This deficit is also visible in Ref. [27], which selects events in FGD2 as well as FGD1.

*Unfolding method*—The Bayesian technique by d’Agostini [30] is used to unfold from the measured reconstructed distributions to the underlying true distributions. For each observable, the true (reconstructed) bins are denoted by  $t_k$  ( $r_j$ ). There are  $n_t$  ( $n_r$ ) true (reconstructed) bins in total. Bayes’ theorem is used to generate the unsmearing matrix

$$P(t_k|r_j) = \frac{P(r_j|t_k)P(t_k)}{\sum_{\alpha=1}^{n_t} P(r_j|t_\alpha)P(t_\alpha)}, \quad (1)$$

where  $P(r_j|t_k)$  is the smearing matrix and  $P(t_k)$  is the Monte Carlo (MC) prior probability of finding a signal event in true bin  $t_k$ . Given a dataset  $N_{r_j}^{\text{meas}}$ , the estimated number of events in each true bin is given by

$$N_{t_k} = \frac{1}{\epsilon_{t_k}} \sum_{j=1}^{n_r} P(t_k|r_j)(N_{r_j}^{\text{meas}} - B_{r_j}), \quad (2)$$

where  $B_{r_j}$  is the number of background events that were selected and  $\epsilon_{t_k}$  is the efficiency of detecting a signal event in bin  $t_k$ . The unfolding is performed separately for each

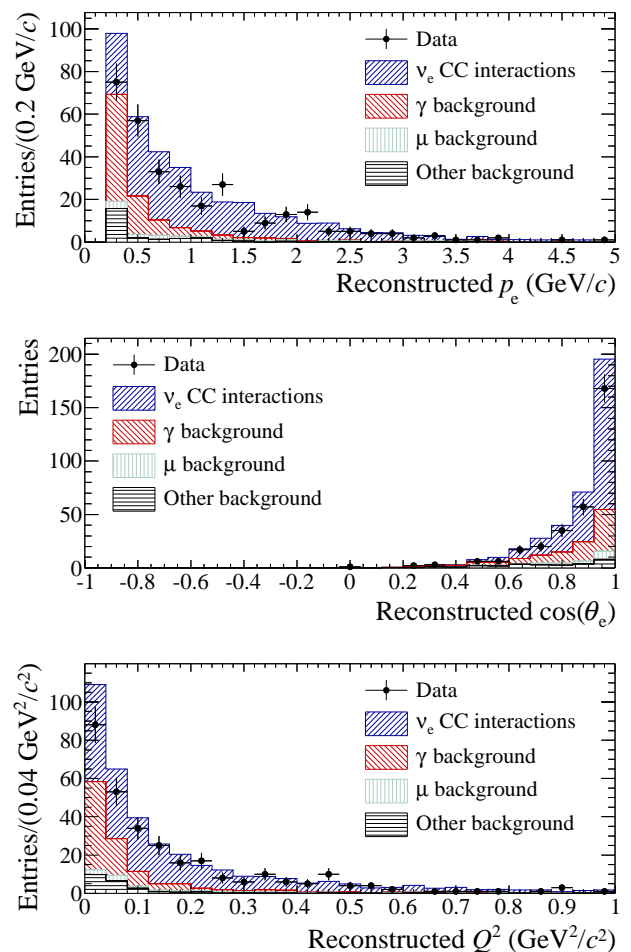


FIG. 1. Reconstructed  $p_e$  (top),  $\cos(\theta_e)$  (middle) and  $Q^2$  (bottom) distributions of  $\nu_e$  event candidates. The NEUT Monte Carlo prediction is separated into the  $\nu_e$  CC interaction signal, background from  $\gamma \rightarrow e^+e^-$  conversions, background from  $\mu^-$  tracks and all other backgrounds. The last bins in the top and bottom plots do not include the overflow of events.

variable. For defining the true bin of each interaction, the true momentum of the electron, true angle of the electron, and true  $Q^2$  of the interaction from the generator are used for  $p_e$ ,  $\cos(\theta_e)$  and  $Q^2$ , respectively. The NEUT neutrino generator is used for the unfolding results presented in this Letter.

The Bayesian unfolding technique was also used in Ref. [6] for measuring the  $\nu_\mu$  CC inclusive cross-section with ND280. The main difference in the unfolding method for this analysis is that the MC background prediction,  $B_{r_j}$ , is estimated using the  $\gamma$  sample. Specifically, the background from neutrino interactions occurring outside of the fiducial volume (out-of-fiducial events) is re-weighted based on the  $\gamma$  sample data. This choice is made as the systematic uncertainties relating to in-fiducial events have been well-studied, 30% of the out-of-fiducial events are on heavy targets (iron and lead)

and 66% are from interaction channels on which there are large uncertainties in the modeling (deep inelastic scattering and neutral current interactions). The MC prediction of events in the fiducial volume is subtracted from the  $\gamma$  sample data, and the data/MC ratio of the out-of-fiducial events is then computed in  $(p_e, \cos(\theta_e))$  bins. The out-of-fiducial component of the  $\nu_e$  sample is re-weighted based on this data/MC ratio distribution. The two-dimensional re-weighting scheme is chosen as the  $\nu_e$  and  $\gamma$  samples preferentially select photons from different origins: the  $\gamma$  sample requires both the  $e^+$  and  $e^-$  to be reconstructed, so preferentially selects higher-energy and more forwards-going photons.

The effect of systematic uncertainties on the cross-section measurements are computed using the same covariance matrix method as in Ref. [6]. Separate covariance matrices are computed for the data statistics, the MC statistics, detector systematics, flux and cross-section systematics, and out-of-fiducial systematics. One thousand toy experiments are performed to generate each matrix, and each experiment simultaneously affects both the  $\nu_e$  and  $\gamma$  samples.

The data statistical uncertainty is evaluated by varying the contents of each data bin according to Poisson statistics. The MC statistical uncertainty is evaluated by separately varying the  $\nu_e$ , the in-fiducial background and the out-of-fiducial background components according to Poisson statistics. Detector systematics are studied by varying parameters such as the momentum resolution, and propagating the effect to the selection. The TPC, FGD, ECal and external interaction uncertainties are described in detail in Ref. [27]. The uncertainty on the FGD mass is 0.67% [6]. The flux and cross-section uncertainties are also described in Ref. [27]. The flux uncertainties are based on beamline measurements and hadron production data. The cross-section uncertainties, including neutrino-nucleon, nuclear modeling, pion production and final state interaction uncertainties are constrained using external data and comparisons between different nuclear models [29]; these uncertainties affect signal efficiencies and background spectra.

Due to the discrepancy between data and MC in the  $\gamma$  sample, conservatively an extra systematic is applied to the out-of-fiducial re-weighting in addition to the statistical uncertainty of the  $\gamma$  sample. If the re-weighting factor in a given bin is  $\alpha$ , then the correction is modeled as a Gaussian with mean  $\alpha$  and width  $\alpha/3$ .

*Cross-section results*—The signal for this analysis is all  $\nu_e$  CC interactions occurring in the FGD1 fiducial volume. FGD1 is composed of carbon (86.1% by mass), hydrogen (7.4%), oxygen (3.7%), titanium (1.7%), silicon (1.0%) and nitrogen (0.1%). The analysis measures the flux-averaged differential  $\nu_e$  CC inclusive cross-section,

and for bin  $t_k$  of variable  $X$ , this is given by

$$\left\langle \frac{\partial \langle \sigma \rangle_\phi}{\partial X} \right\rangle_{t_k} = \frac{N_{t_k}}{\Delta X_{t_k} T \phi}, \quad (3)$$

where  $X$  is either  $p_e$ ,  $\cos(\theta_e)$  or  $Q^2$ ,  $\Delta X_{t_k}$  is the width of the bin,  $N_{t_k}$  is the total number of signal events in the bin,  $T$  is the number of target nucleons ( $5.5 \times 10^{29}$  [6]),  $\phi$  is the total integrated flux ( $1.35 \times 10^{11} \text{ cm}^{-2}$ ), and  $\langle \dots \rangle_\phi$  indicates that the quantity is averaged over the flux.

The total flux averaged cross-section per nucleon is computed by summing over all  $X$  bins, as

$$\langle \sigma \rangle_\phi = \frac{\sum_{k=1}^{n_t} N_{t_k}}{T \phi}. \quad (4)$$

For comparison, differential and total flux-averaged cross-section predictions are computed using the NEUT (version 5.1.4.2) and GENIE (version 2.6.4 [31]) generators.

Fig. 2 shows the unfolded differential cross-section results as a function of  $p_e$ ,  $\cos(\theta_e)$  and  $Q^2$ . The data agrees with both NEUT and GENIE, although a deficit is seen at low  $Q^2$  compared to NEUT. The biggest differences between NEUT and GENIE at low  $Q^2$  are caused by the different values of  $M_A^{QE}$  chosen for CCQE interactions, and different CC coherent interaction models.

The total flux-averaged cross-section when unfolding through  $Q^2$  is  $\langle \sigma \rangle_\phi = 1.11 \pm 0.09$  (stat)  $\pm 0.18$  (syst)  $\times 10^{-38} \text{ cm}^2/\text{nucleon}$ , which agrees with both the NEUT prediction of  $1.23 \times 10^{-38} \text{ cm}^2/\text{nucleon}$  and the GENIE prediction of  $1.08 \times 10^{-38} \text{ cm}^2/\text{nucleon}$ . The result is shown in Fig. 3, along with the Gargamelle data from 1978 [9]. The results when unfolding through the other variables agree at the percent level. The dominant systematic uncertainties on this result are the flux (12.9%) and detector systematics (8.4%), with all other systematics giving a 6.1% uncertainty when added in quadrature. The uncertainty from re-weighting the out-of-fiducial background is 2.1%.

An important aspect of the Bayesian unfolding approach is that it allows a reconstructed distribution to be unfolded into regions that it is not sensitive to. This analysis has poor reconstruction efficiency for low momentum, backwards going, or high angle electrons. This adds model dependency since the NEUT generator must predict these poorly determined regions. For this reason, a second result is presented, in which only events with  $p_e > 550 \text{ MeV}$  and  $\cos(\theta_e) > 0.72$  are considered. In this “reduced phase-space” result, no attempt is made to unfold into regions of low detector efficiency. The unfolded  $Q^2$  differential cross-section result for this reduced phase-space is shown in Fig. 4.

*Conclusion*—Understanding differences between  $\nu_e$  and  $\nu_\mu$  cross-sections is vital as long baseline oscillation experiments search for CP violation in the lepton sector. The T2K off-axis near detector, ND280, has been

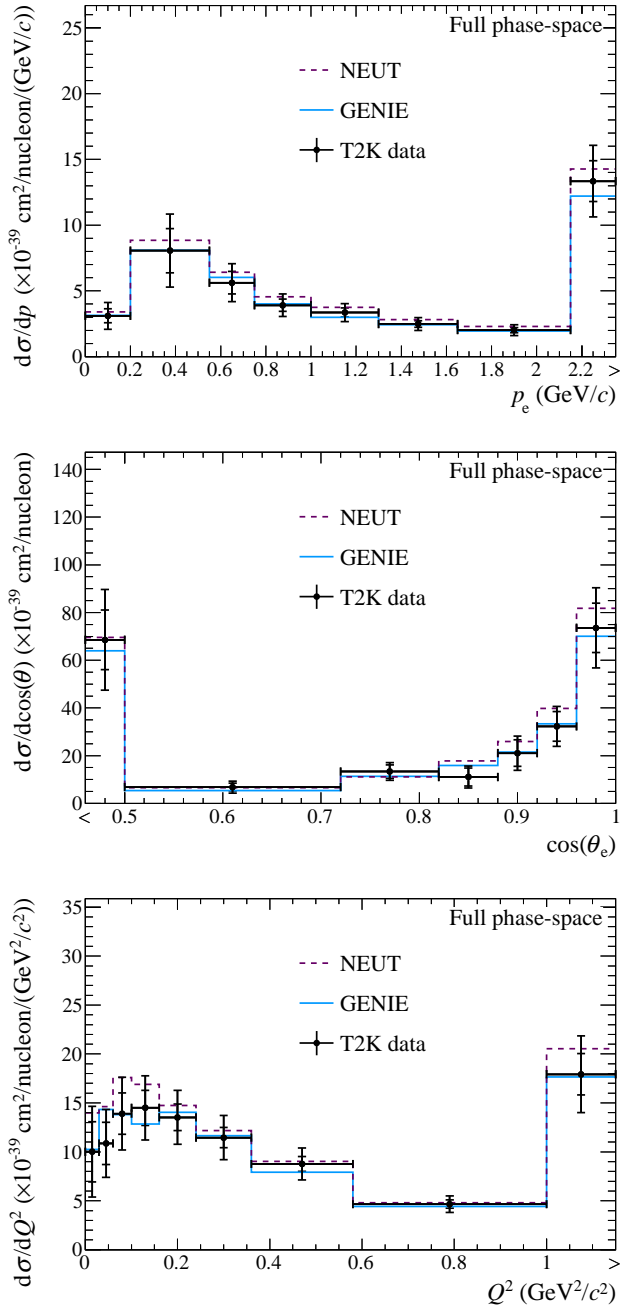


FIG. 2. Unfolded  $\nu_e$  CC inclusive differential cross-sections as a function of  $p_e$  (top),  $\cos(\theta_e)$  (middle) and  $Q^2$  (bottom). The inner (outer) error bars show the statistical (total) uncertainty on the data. The dashed (solid) line shows the NEUT (GENIE) prediction. Overflow (underflow) bins are indicated by  $>$  ( $<$ ) labels, and are normalized to the width shown.

used to extract  $\nu_e$  CC inclusive flux-averaged differential cross-sections as a function of  $p_e$ ,  $\cos(\theta_e)$  and  $Q^2$ , and they are found to agree with both the NEUT and GENIE neutrino interaction generator predictions. These are the first ever  $\nu_e$  differential cross-section measurements at the GeV-scale. The total  $\nu_e$  CC inclusive flux-averaged cross-

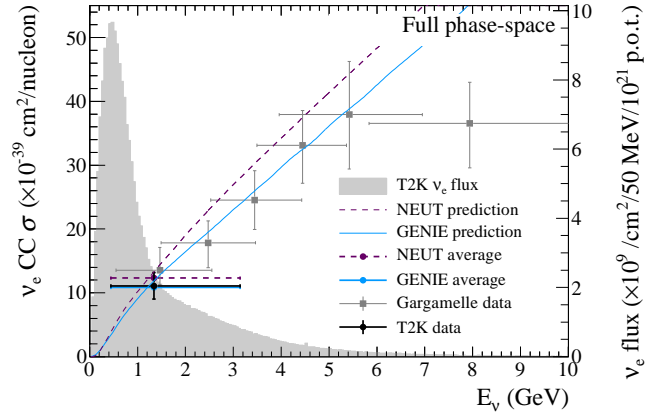


FIG. 3. Total  $\nu_e$  CC inclusive cross-section when unfolding through  $Q^2$ . The T2K data point is placed at the  $\nu_e$  flux mean energy. The vertical error represents the total uncertainty, and the horizontal bar represents 68% of the flux each side of the mean. The T2K flux distribution is shown in grey. The NEUT and GENIE predictions are the total  $\nu_e$  CC inclusive predictions as a function of neutrino energy. The NEUT and GENIE averages are the flux-averaged predictions. The Gargamelle data is taken from Ref. [9].

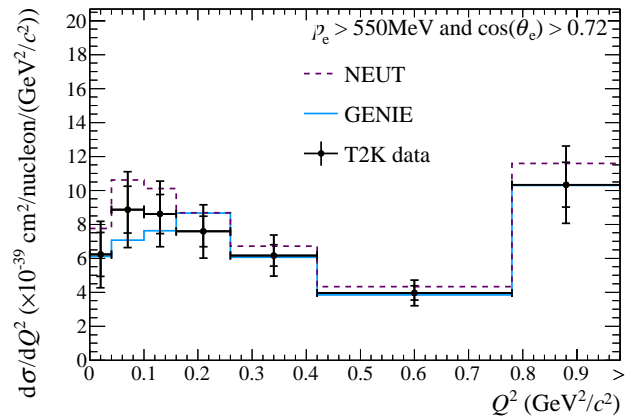


FIG. 4. Unfolded  $\nu_e$  CC inclusive differential cross-section as a function of  $Q^2$ , when only electrons with  $p_e > 550$  MeV and  $\cos(\theta_e) > 0.72$  are considered. The inner (outer) error bars show the statistical (total) uncertainty on the data. The dashed (solid) line shows the NEUT (GENIE) prediction. Overflow (underflow) bins are indicated by  $>$  ( $<$ ) labels, and are normalized to the width shown.

section is found to be  $1.11 \pm 0.20 \times 10^{-38}$  cm<sup>2</sup>/nucleon, which is also in agreement with the NEUT and GENIE predictions. The data related to the measurement can be found in [32].

We thank the J-PARC staff for superb accelerator performance and the CERN NA61 collaboration for providing valuable particle production data. We acknowledge the support of MEXT, Japan; NSERC, NRC, and CFI, Canada; CEA and CNRS/IN2P3, France; DFG,

Germany; INFN, Italy; National Science Centre (NCN), Poland; RAS, RFBR, and MES, Russia; MICINN and CPAN, Spain; SNSF and SER, Switzerland; STFC, UK; and DOE, USA. We also thank CERN for the UA1/NOMAD magnet, DESY for the HERA-B magnet mover system, NII for SINET4, the WestGrid and SciNet consortia in Compute Canada, GridPP, UK, and the University of Oxford Advanced Research Computing (ARC) facility. In addition participation of individual researchers and institutions has been further supported by funds from: ERC (FP7), EU; JSPS, Japan; Royal Society, UK; DOE Early Career program, USA.

---

\* also at J-PARC, Tokai, Japan

† also at Institute of Particle Physics, Canada

‡ affiliated member at Kavli IPMU (WPI), the University of Tokyo, Japan

§ also at Moscow Institute of Physics and Technology and National Research Nuclear University "MEPhI", Moscow, Russia

¶ also at JINR, Dubna, Russia

\*\* deceased

†† also at BMCC/CUNY, Science Department, New York, New York, U.S.A.

- [1] B. M. Pontecorvo, *JETP Lett.* **33**, 549 (1957).
- [2] Z. Mäki, M. Nakagawa, and S. Sakata, *Prog. Theor. Phys.* **28**, 870 (1962).
- [3] J. Beringer *et al.* (Particle Data Group), *Phys. Rev. D* **86**, 010001 (2012).
- [4] K. Abe *et al.* (T2K Collaboration), *Phys. Rev. Lett.* **112**, 061802 (2014).
- [5] J. A. Formaggio and G. P. Zeller, *Rev. Mod. Phys.* **84**, 1307 (2012).
- [6] K. Abe *et al.* (T2K Collaboration), *Phys. Rev. D* **87**, 092003 (2013).
- [7] B. Tice *et al.* (MINERvA Collaboration), Submitted to *Phys. Rev. Lett.* (2014), arXiv:1403.2103.
- [8] G. Fiorentini *et al.* (MINERvA Collaboration), *Phys. Rev. Lett.* **111**, 022502 (2013).
- [9] J. Blietschau *et al.* (Gargamelle Collaboration), *Nucl. Phys.* **B133**, 205 (1978).
- [10] M. Day and K. S. McFarland, *Phys. Rev. D* **86**, 053003 (2012).
- [11] K. Abe *et al.* (T2K Collaboration), *Nucl. Instrum. Methods* **A659**, 106 (2011).
- [12] K. Matsuoka *et al.*, *Nucl. Instrum. Methods* **A624**, 591 (2010).
- [13] M. Otani *et al.*, *Nucl. Instrum. Methods* **A623**, 368 (2010).
- [14] S. Fukuda *et al.* (Super-Kamiokande Collaboration), *Nucl. Instrum. Methods* **A501**, 418 (2003).
- [15] P. Amaudruz *et al.* (T2K ND280 FGD Collaboration), *Nucl. Instrum. Methods* **A696**, 1 (2012).
- [16] N. Abgrall *et al.* (T2K ND280 TPC Collaboration), *Nucl. Instrum. Methods* **A637**, 25 (2011).
- [17] S. Assylbekov *et al.* (T2K ND280 P0D Collaboration), *Nucl. Instrum. Methods* **A686**, 48 (2012).
- [18] D. Allan *et al.* (T2K UK Collaboration), *JINST* **8**, P10019 (2013).
- [19] S. Aoki *et al.* (T2K ND280 SMRD Collaboration), *Nucl. Instrum. Methods* **A698**, 135 (2013).
- [20] K. Abe *et al.* (T2K Collaboration), *Phys. Rev. D* **87**, 012001 (2013).
- [21] A. Ferrari, P. Sala, A. Fasso, and J. Ranft, *FLUKA: A Multi-Particle Transport Code* (2005).
- [22] N. Abgrall *et al.* (NA61/SHINE Collaboration), *Phys. Rev. C* **84**, 034604 (2011).
- [23] N. Abgrall *et al.* (NA61/SHINE Collaboration), *Phys. Rev. C* **85**, 035210 (2012).
- [24] R. Brun, F. Carminati, and S. Giani, CERN-W5013 (1994).
- [25] C. Zeitnitz and T. A. Gabriel, In Proc. of International Conference on Calorimetry in High Energy Physics (1993).
- [26] K. Abe *et al.* (T2K Collaboration), *Nucl. Instrum. Methods* **A694**, 211 (2012).
- [27] K. Abe *et al.* (T2K Collaboration), *Phys. Rev. D* **89**, 092003 (2014).
- [28] Y. Hayato, *Nucl. Phys. Proc. Supp.* **B112**, 171 (2002).
- [29] K. Abe *et al.* (T2K Collaboration), *Phys. Rev. D* **88**, 032002 (2013).
- [30] G. D'Agostini, *Nucl. Instrum. Methods* **A362**, 487 (1995).
- [31] C. Andreopoulos *et al.*, *Nucl. Instrum. Methods* **A614**, 87 (2010).
- [32] K. Abe *et al.*, "T2K public data," <http://t2k-experiment.org/results/nd280-nue-xs-2014>.